Biochimica et Biophysica Acta 1828 (2013) 758–764

Contents lists available at SciVerse ScienceDirect

Biochimica et Biophysica Acta

journal homepage: www.elsevier.com/locate/bbamem

The defensin–lipid interaction: Insights on the binding states of the human antimicrobial peptide HNP-1 to model bacterial membranes

Alessio Bonucci [a], Enrico Balducci [b], Sara Pistolesi [c], Rebecca Pogni [a,*]

[a] Department of Chemistry, University of Siena, 53100 Siena, Italy
[b] School of Biosciences and Biotechnology, University of Camerino, 62032 Camerino, Italy
[c] Laboratory of Molecular Biophysics, National Heart, Lung, and Blood Institute, National Institutes of Health, Bethesda, MD, 20892, USA

ARTICLE INFO

Article history:
Received 17 July 2012
Received in revised form 8 October 2012
Accepted 8 November 2012
Available online 15 November 2012

Keywords:
HNP-1
Antimicrobial peptide
Bacterial model membrane
Bilayer interaction
Spectroscopic analysis
Partition coefficient

ABSTRACT

Antimicrobial peptides are an important component of innate immunity and have generated considerable interest as a new potential class of natural antibiotics. The biological activity of antimicrobial peptides is strongly influenced by peptide–membrane interactions. Human Neutrophil Peptide 1 (HNP-1) is a 30 aminoacid peptide, belonging to the class of α-defensins. Many biophysical studies have been performed on this peptide to define its mechanism of action. Combining spectroscopic and thermodynamic analysis, insights on the interaction of the α-defensin with POPE:POPG:CL negative charged bilayers are given. The binding states of the peptide below and above the threshold concentration have been analyzed showing that the interaction with lipid bilayers is dependent by peptide concentration. These novel results that indicate how affinity and biological activities of natural antibiotics are depending by their concentration, might open new way of investigation of the antimicrobial mode of action.

1. Introduction

A wide variety of organisms produces antimicrobial peptides (AMPs) as part of their first line of defence [1]. AMPs are typically relatively short (12 to 100 amino acids), positively charged (net charge ranging from +2 to +9, with +4 to +6 being the most common) and contain about ~50–70% of hydrophobic amino acids [1–5]. AMPs display a broad spectrum of antimicrobial activity against both Gram-positive and Gram-negative bacteria, fungi, yeast and enveloped viruses [6].

It is believed that the mechanism of antimicrobial action is related to the permeabilization of the microbial cell membrane [6,7]. In this context the lipid composition is a key factor to better understand the peptide:lipid interaction in model membranes [5–7]. Several models have been proposed to describe the molecular events involved in the AMP-mediated membrane disruption, including the formation of barrel-stave peptide channels, induction of peptide–lipid toroidal pores and a detergent-like mechanism [2–8]. The threshold concentration of AMPs is an important factor to understand their mechanism of action. Generally, the interaction between peptides and lipids takes place in two steps: deposition on the membrane surface and insertion into the bilayer. At exceeding threshold concentrations, all peptides are able to destabilize the phospholipid bilayer and cause membrane disruption [7,9–13]. For this reason, it is likely that some results for putative AMPs permeabilizing vesicles are essentially artefacts that arise from extremely high peptide:lipid ratios used. In general, any membrane-interacting molecule can disrupt membranes at very high concentrations.

Human Neutrophil Peptide 1 (HNP-1) is a peptide belonging to the class of α-defensins, which are produced in azurophil granules of neutrophils [14]. This 30 amino acid peptide is present as a dimer in solution. Each monomer unit is composed of three anti-parallel β-sheet and a β-hairpin. The peptide structure is strongly stabilized by three cysteine disulfide bridges (C_2–C_{30}, C_4–C_{19}, C_9–C_{29}) interconnecting each β-sheet and a salt bridge between Arg-5 and Glu-13 [15]. HNP-1 has a positive net charge equal to +3, conferred by four cationic arginine residues and the single anionic glutamic acid residue [16–18]. The general mechanism for its antimicrobial action relies on the permeabilization of the microbial cell membrane [19,20] and the importance of Arg and Trp residues of HNP-1 for this membrane interaction is now clear [21–24]. A "dimer pore" model for HNP-1 has been suggested on the basis of a crystal structure study [25], while a multimeric pore model was proposed on the basis of vesicle leakage and dextran permeability experiments [26].

Abbreviations: AMP, antimicrobial peptide; HNP-1, human neutrophil peptide 1; EPR, Electron Paramagnetic Resonance; CD, Circular Dichroism; POPG, 1-palmitoyl-2-oleoyl-*sn*-glycerol-3-phosphatidylglycerol; POPE, 1-palmitoyl-2-oleoyl-*sn*-glycerol-3-phosphatidylethanolamine, CL, 1,1′,2,2′-tetramyristoyl cardiolipin ammonium salt; MOPS, 3-(N-morpholino) propanesulfonic acid; LUV, Large Unilamellar Vesicle; PCSL, phosphatidylcholine spin-labels; DMPC:DMPG, 1,2-dimyristoyl-*sn*-glycero-3-phosphocholine:1,2-dimyristoyl- *sn*-glycero-3-phosphatidylglycerol

* Corresponding author at: Department of Chemistry, University of Siena, Via A. de Gasperi 2, 53100 Siena, Italy. Tel.: +39 0577 234258; fax: +39 0577 234239.
E-mail address: rebecca.pogni@unisi.it (R. Pogni).

0005-2736/$ – see front matter © 2012 Elsevier B.V. All rights reserved.
http://dx.doi.org/10.1016/j.bbamem.2012.11.011

In this study, a combined approach using spectroscopic (EPR, CD and Fluorescence) and thermodynamic techniques have been used to analyze the binding states of the HNP-1 peptide with POPE:POPG:CL liposomes as it accumulates on the bilayer surface. The peptide:lipid 1:20 molar ratio has been determined as the threshold concentration at which the peptide penetrates into the bilayer. When the α-defensin:lipid molar ratio is above or below the threshold concentration, the peptide tends to accumulate on the membrane surface with a different mechanism of action.

2. Material and methods

The HNP-1 peptide [ACYCRIPACIAGERRYGTCIYQGRLWAFCC] was obtained from Bachem Peptide (Bubendorf, CH) and used without further purification. The phospholipids for vesicle preparation, 1-palmitoyl-2oleoyl-*sn*-glycerol-3-phosphoglycerol (POPG), 1-palmitoyl-2oleoyl-*sn*-glycerol-3-phosphoethanolamine(POPE), 1,1′,2,2′-tetramyristoyl cardiolipin ammonium salt (CL), and spin-labeled phosphatidylcholine (1-acyl-2-[*n*-(4,4dimethyloxazolidinyl-N-oxyl)]stearoyl-*sn*-glycero-3-phosphocholine, *n*-PCSL, with n = 5, 7, 12) were obtained from Avanti Polar Lipids (Alabaster, AL). The buffer solution (pH 6.8) used in the experiments contains 50 mM of 3-(N-morpholino) propanesulfonic acid (MOPS) (Sigma Aldrich). MOPS is a buffer largely used for biological sample preparation due to its low salt content [27].

2.1. Liposome preparation

Liposomes were prepared mixing 14 mM POPE, 12.9 mM POPG and 6.6 mM CL (POPE:POPG:CL 70:25:5 molar ratio), in agreement with the composition of Gram-negative bacterial inner membrane lipids [13,28].

Lipids at the desired molar ratio were dried down from chloroform stock solutions under a stream of nitrogen gas and then dried under vacuum for 1 h. The resulting lipid film was hydrated by adding 50 mM MOPS at pH 6.8 to reach a final concentration of about 50 mM phospholipids. Large unilamellar vesicles (LUVs) were prepared by freeze-thawing this lipid suspension five times followed by extrusion through 200 nm polycarbonate membrane filters using a miniextruder syringe device (Avanti Polar Lipids). Final concentration of LUVs was determined using the Stewart phospholipids assay [29]. LUVs containing 1 mol of 5, 7, or 12-PCSL were prepared as described above. Different peptide:lipid molar ratios were prepared (1:5, 1:10, 1:15, 1:20, 1:30, 1:50, 1:100, 1:250 and 1:350) where the HNP-1 peptide was incubated with LUVs in 50 mM MOPS buffer at pH 6.8 for 1 h.

2.2. Circular dichroism spectroscopy

CD experiments were performed at room temperature on a Jasco CD-J-815 spectropolarimeter using a quartz cuvette with a path length of 1 mm. Peptide was suspended at 0.02 mM concentration in 50 mM MOPS at pH 6.8 with a variable concentration of LUVs ranging from 0.1 to 7 mM. CD spectra were recorded from 190 to 250 nm and accumulated ten times to improve the signal-to-noise ratio. Baselines of either solvent or vesicular suspension without peptide were subtracted from each respective sample to calculate the peptide contribution [30].

2.3. Electron Paramagnetic Resonance spectroscopy

EPR spectra were recorded on a Bruker E500 ELEXSYS X-Band spectrometer equipped with a super-high-Q cavity. Samples prepared for EPR measurements contained 0.4 mM of *n*-PCSL LUVs and a variable concentration of peptide ranging from 0.02 to 0.08 mM. Spectra were recorded using the following instrumental settings: 120 G sweep width; 100 kHz modulation frequency; 1.0 G modulation amplitude; 40 ms time constant; 20 mW microwave power. Several scans, generally 15, were made to improve the signal-to-noise ratio. Values of the outer hyperfine splitting, $2A_{max}$, were determined by measuring the difference between the low-field maximum and minimum. Measurements were performed in triplicate and the reproducibility of $2A_{max}$ is typically ±0.02–0.07 G. The relative values of $2\Delta A_{max}$ were obtained by calculating the difference of outer hyperfine splitting constant for the spectra with or without HNP-1. To assess the rotational mobility of 12-PCSL, the apparent rotational correlation time (τ) was determined according to [13]:

$$\tau = \left(0.65 \cdot 10^{-9}\right) \Delta H_0 \left[\left(A_0/A_{-1}\right)^{1/2} - 1\right] \quad (1)$$

where ΔH_0 is the peak-to-peak width of the center line in gauss, A_0 is the amplitude of the center line, and A_{-1} is the amplitude of the high field line (see Fig. 2). The rotational correlation time is inversely related to the motional spin label rate such that an increase in τ indicates slower motion.

2.4. Fluorescence and thermodynamic measurements

Peptide–lipid interactions were studied by monitoring the change in the Trp-26 fluorescence emission spectra in the presence of LUVs. Samples prepared for fluorescence measurements contained 0.02 mM peptide and a variable phospholipids concentration ranging from 0.1 to 7 mM. Fluorescence measurements were performed on a Jasco FB-6500 spectrometer. The excitation wavelength was 280 nm, and emission spectra were recorded between 290 and 400 nm, with a 1 nm slit widths at room temperature [31,32]. A very small emission band in the range of 290–310 nm due to tyrosine residues contribution is present in some samples, but it does not influence the tryptophan fluorescence band [33].

Binding experiments of peptide to LUVs (0.02 mM HNP-1 in 50 mM MOPS buffer at pH 6.8) were performed with an ultrafiltration assay to separate lipid phase from the free peptide using Centricon-30 kDa cut-off filters (Millipore Inc.). The peptide was added to LUVs at a peptide:lipid molar ratio of 1:350, 1:250, 1:100, 1:50, 1:30, , 1:20, 1:15, 1:10, 1:5, incubated for 30 min and then centrifuged at 6000 × *g* for 1 h [36].

The free peptide concentration in the eluate has been determined through a calibration curve plotting known peptide concentration versus fluorescence intensity. The amount of the peptide bound to lipid was measured by subtracting the free peptide concentration from the total peptide concentration. Based on our CD studies, we found that α-defensin can form aggregates in solution at physiological pH at a concentration above 0.04 mM (data not shown). In all partition coefficient experiments, HNP-1 concentration has been maintained below 0.04 mM to avoid peptide aggregation process that could bring to a misleading determination of free protein concentration.

The mole fraction partition coefficient (K_p) was determined as following:

$$K_p = \left([P]_{bilayer}/[L]\right)/\left([P]_{wat}/[W]\right) \quad (2)$$

where [P] is the peptide concentration in the bilayer or water phase, [L] is the molar lipid concentration and [W] is the water molar concentration (55.3 M at 25 °C). The free energies of transfer, ΔG°, from water to lipid were calculated from:

$$\Delta G^\circ = -RT \ln K_p \quad (3)$$

where R is the gas constant and T is the temperature [34–36].

For quenching experiments, samples were prepared dissolving HNP-1 in 50 mM MOPS (pH = 6.8) at a final concentration of 0.02 mM. Vesicles were added in specific peptide:lipid molar ratio equal to 1:5,

1:20 and 1:250. After an incubation of about 30 min, 2 mM potassium iodide (KI) was added and fluorescence spectra were recorded.

For doxyl-PCSL quenching experiments, spin labeled LUVs were prepared with the same protocol of the EPR spectroscopic analysis. n-PCSL-LUVs were added to a solution containing 0.02 mM HNP-1 in 50 mM MOPS (pH = 6.8) to give 1:250, 1:20 and 1:5 peptide: lipid molar ratios, respectively. Each sample was incubated at room temperature for almost 30 min and fluorescence emission spectra were recorded before and after the incubation time as described [37,38]. For both analysis, quenching effect was calculated as the ratio between the intensity of fluorescence spectra in the presence and in the absence of the quencher (i.e. KI or doxyl-PCSL) for each specific peptide:lipid ratio. Fluorescence spectra were recorded with Jasco FB-6500 spectrometer using the same setting as previously described.

3. Results

3.1. Circular dichroism spectroscopy

Conformational changes of HNP-1 were investigated by CD spectroscopy in solution and in the presence of model membranes (Fig. 1). The native HNP-1 (Fig. 1 *open circles*) shows a negative band at ~205 nm and a cross over around 200 nm. The observed bands represent protein containing β-hairpin secondary structure and some low percentages of α-helical contribution (12%) [39,40].

For low peptide:lipid molar ratio (1:250), the CD spectrum shows again the classical absorbance around 205 nm due to the β-hairpin (Fig. 1 *solid squares*). Increasing peptide concentrations (1:20 and 1:5), a change in terms of molar ellipticity and shape of the absorbance band has been observed (Fig. 1 *closed circles* and *triangles* respectively). CD spectrum for the 1:20 ratio (Fig. 1 *solid triangles*) shows positive band at 198 nm and negative band at 215 nm with a β-sheet lineshape. For 1:5 ratio (Fig. 1 *solid circles*), the spectrum is characterized by a single minimum at ~215 nm typical of a β-sheet structure but no cross-over is revealed. Probably high peptide concentration could determine peptide–lipid aggregation causing spectral distortion.

3.2. Emission fluorescence spectroscopy

Changes in Trp fluorescence have been used as a probe to monitor variations in the local hydrophobic environment of a protein or peptide. In this context HNP-1 contains a single tryptophan residue (Trp-26). Fig. 2 displays the tryptophan emission spectra of HNP-1 in solution

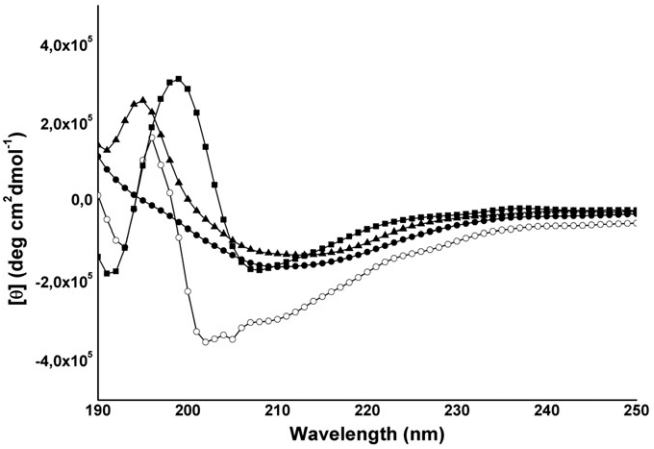

Fig. 1. Circular dichroism spectra (190–250 nm range) of HNP-1 in 50 mM MOPS buffer (*open circles*) and in the presence of LUVs at peptide:lipid molar ratio 1:250 (*squares*), 1:20 (*triangles*) and 1:5 (*solid circles*). Baselines of either solvent or vesicular suspension without peptide have been subtracted from each sample. Spectral distortion is present below 195 nm. Data are representative of three independent experiments.

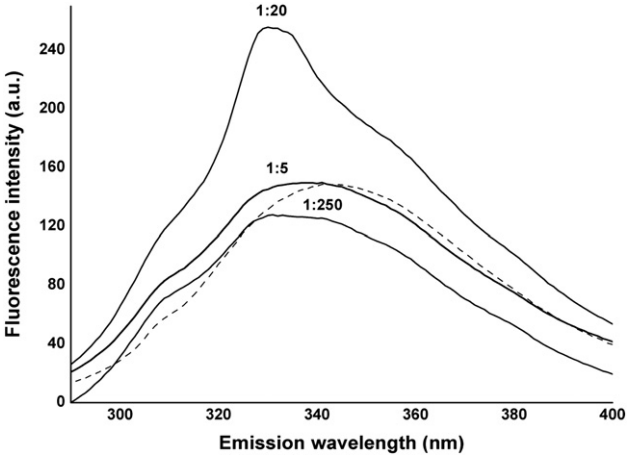

Fig. 2. Trp emission spectra (range 290–400 nm) of HNP-1 in 50 mM MOPS buffer (*dotted line*) and in the presence of LUVs at peptide:lipid molar ratios of 1:250,1:20 and 1:5. The excitation wavelength was 280 nm. The spectra were recorded at room temperature. Experiments repeated three times gave similar results.

and in the presence of different amounts of negatively charged liposomes. A blue shift and a variation in quantum yield are typical features of when a Trp residue moves from water to an apolar environment [32]. The maximum emission of HNP-1 at 343 nm (Fig. 2 *dotted line*), is typical of a peptide containing an indole moiety. Adding a large amount of lipid phase to reach 1:250 peptide:lipid ratio a decrease in fluorescence quantum yield accompanied by blue shift of the emission band is evident (Fig. 2). The change in quantum yield is in the opposite direction from lower (1:250) to higher (1:20) peptide:lipid molar ratios (Fig. 2) indicating a different mechanism of interaction. The blue shift of the band and the enhancement of the fluorescence quantum yield for 1:20 ratio indicates that the tryptophan is located in an apolar space [31,32]. Interestingly, when reached 1:5 peptide:lipid molar ratio the blue shift is maintained while the fluorescence intensity of Trp-26 returns at the same intensity of that of the free peptide in solution. This trend suggests a different partitioning mechanism of HNP-1 with the lipid bilayer.

3.3. Electron Paramagnetic Resonance measurements

The EPR technique has been proved to be a powerful tool to monitor the peptide–membrane interaction using site-specific spin-labeled lipids [13,41–44].

To assess the effects of the HNP-1 interaction with lipid membranes, the motion of phosphatidylcholine spin labels with the nitroxide moiety positioned at various depths along the alkyl chain has been examined. CW-EPR spectra for 5-, 7- and 12-PCSL in POPE:POPG:CL (70:25:5) LUVs with and without HNP-1 are shown in Fig. 3. The increase in $2A_{max}$ reflects the selectivity of the interaction with lipid head-groups and also the different strengths of lipid interaction with the peptide.

Fig. 4 shows the increase of $2\Delta A_{max}$ for 5- (squares) and 7-PCSL (circles) rising peptide:lipid molar ratio. The most pronounced patterns of selectivity and the largest degrees of perturbation (i.e., largest values of $2\Delta A_{max}$) are obtained adding 1:5 and 1:10 HNP-1 to LUV membranes ($2\Delta A_{max} = 2.54 \pm 0.07$ G and $2\Delta A_{max} = 2.75 \pm 0.07$ G, respectively), while for the other ratios a strong decrease of about 80% is observed for 5-PCSL. A similar trend is observed for 7-PCSL, although changes are smaller than for 5-PCSL. Table 1 gives the values of $2\Delta A_{max}$recorded for various peptide:lipid molar ratios for 5- and 7-PCSL.

Since 12-PCSL undergoes more rapid motion than 5- or 7-PCSL, the outer splitting constant ($2A_{max}$) is less sensitive to changes in mobility than the width of the center line (ΔH_0) or relative line amplitudes, which can be used to calculate an empirical rotational

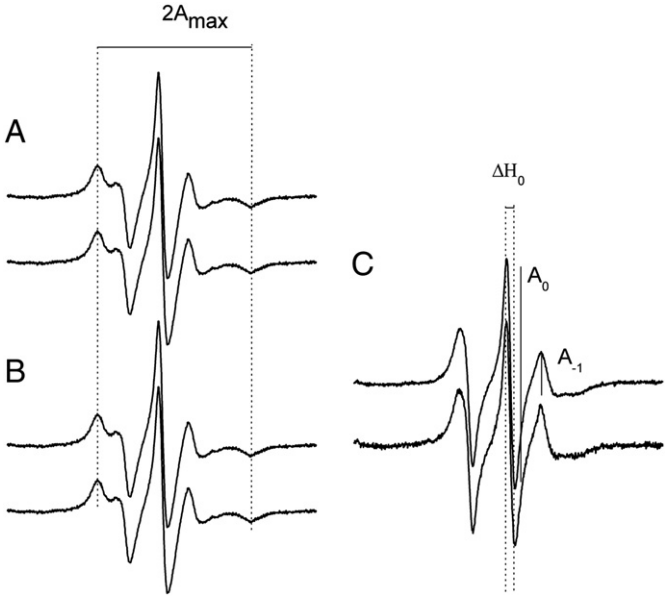

Fig. 3. EPR spectra of 5-PCSL (A), 7-PCSL (B) and 12-PCSL (C) positional isomers of spin -labeled phosphatidylcholine in fluid-phase LUVs, with (*upper spectrum*) and without (*lower spectrum*) HNP-1 for 1:20 peptide:lipid molar ratio. The increase in $2A_{max}$ observed for 5- and 7-PCSL indicates a decrease in rotational mobility. For 12PCSL the rotational correlation time is inversely related to the motional spin label rate. Scan widths are 120 G, modulation amplitude 1.0 G. Shown is a typical experiment out of three.

correlation time, τ (see Material and methods and Fig. 3). For 12-PCSL, variation in peptide concentration does not produce significant changes in ΔH_0 and rotational correlation time (τ) except for the 1:20 peptide:lipid molar ratio (Table 2).

3.4. Partition coefficient measurements

Fluorescence measurements can also be conveniently used to calculate the partitioning equilibrium of the peptide into LUVs. Partition coefficient (K_p) and insertion free energy of various peptide:lipid molar ratios were determined as described in the Material and methods section and data are summarized in Table 3. As shown in Fig. 5, the increase in K_p has been recorded accordingly to the amount of added liposomes. For low peptide:lipid molar ratio (from 1:350 to 1:100), the lowest values of the partition coefficient indicate a weak interaction of peptide

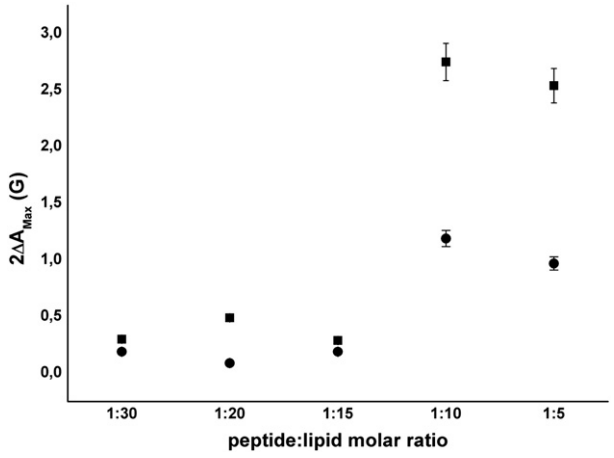

Fig. 4. Difference in the outer hyperfine splittings ($2\Delta A_{max}$) of *n*-PCSL, 5-PCSL (*squares*) and 7-PCSL (*circles*) for different HNP-1:LUV ratios. Error bars indicate standard deviations from three different measurements.

Table 1
Differences in outer hyperfine splittings ($2\Delta A_{max}$) of phospholipid probes, for 5-PCSL and 7-PCSL, incorporated in LUVs at different peptide:lipid molar ratios.

Pep:lip molar ratio	5-PCSL	7-PCSL
	2ΔAmax ± 0.07 G	2ΔAmax ± 0.06 G
1:30	0.30	0.19
1:20	0.49	0.09
1:15	0.29	0.19
1:10	2.75	1.19
1:5	2.54	0.97

with the lipid phase. For 1:15 and 1:20 peptide:lipid molar ratios, there is a strong increase of K_p values. For 1:20 peptide:lipid molar ratio, HNP-1 is prevalently associated with the phospholipid bilayer. The relative partition coefficient is higher than all the other ratios and it is related to a lower value of free energy. The mole-fraction partition coefficient for 1:5 HNP-1:LUVs ratio is $0.37\times10^3\pm5\%$. This yields a water-to-bilayer free energy transfer of $\Delta G^\circ = -3.51\pm0.3$ kcal/mol while for the 1:20 molar ratio a value of $K_p = 0.68\times10^3\pm5\%$ and $\Delta G^\circ = -3.85\pm0.3$ kcal/mol have been determined. These results show a strong interaction with the bilayer for the 1:20 peptide:lipid molar ratio while for the other ratios weaker interactions can be revealed.

3.5. Tryptophan quenching experiments

Potassium iodide (KI) can be used to determine the water exposure of tryptophan residues. If the residue is solvent exposed, iodide quenches its fluorescence emission. In Table 4 the values of KI quenching expressed as ratio between the fluorescence intensity in the presence and in the absence of the quencher for three specific peptide:lipid molar ratios are reported. The maximum KI quenching is found for 1:250 ratio, suggesting that HNP-1 is largely exposed to buffer. For the other two ratios, the Trp-26 is more localized into the bilayer.

To determine the depth of HNP-1 penetration into LUVs, doxyl-quenching experiments have been performed using the same spin-labeled membranes adopted in the EPR experiments. The doxyl radical anchored at different positions of the phospholipid tails (i.e. 5, 7 and 12 carbon of PC lipid) can quench the Trp-26 fluorescence when peptide approaches the lipid bilayer. For low peptide: lipid molar ratio (1:250) only the doxyl linked to 5 carbon of PC lipid quenches the Trp-26 fluorescence, indicating a superficial peptide interaction. The well pronounced quenching that occurs at 1:20 peptide:lipid ratio is consistent with peptide penetration into the middle hydrocarbon space of lipid bilayer. On the other hand, for the highest peptide:lipid molar ratio tested (1:5) the maximum value of doxyl-quenching is relative to 5- and 7-PCSL indicating that HNP-1 is inserted into vesicles but interacts prevalently with the outer part of membrane (Table 4).

Table 2
Motional parameters for 12-PCSL incorporated in LUVs as a function of peptide:lipid molar ratio.

Pep:lip molar ratio	$\Delta H_0 \pm 0.02$ G [a]	$\tau \pm 0.07$ ns[b]
0:1	2.76	2.31
1:30	2.77	2.36
1:20	2.86	2.44
1:15	2.76	2.38
1:10	2.73	2.28
1:5	2.71	2.31

Mean ± standard error of the [a]peak–peak width of the center line (ΔH_0) and rotational [b]correlation time (τ) are from three different experiments.

Table 3
[a] Partition coefficients and [b] free energies of HNP-1 into LUVs determined at various peptide:lipid molar ratios. The wavelength range of 330–340 nm has been used to calculate the amount of free peptide in solution.

Pep:lip molar ratio	$K_p \cdot 10^{-3} \pm 5\%$[a]	$\Delta G° \pm 0.3$ kcal/mol [b]
1:350	0.07	−2.44
1:250	0.02	−1.87
1:100	0.04	−2.12
1:50	0.11	−2.76
1:30	0.34	−3.40
1:20	0.68	−3.85
1:15	0.62	−3.78
1:10	0.35	−3.46
1:5	0.37	−3.51

Table 4
Measurements of Trp fluorescence quenching to determine penetration depth of peptide into lipid bilayer and water exposed indole moiety.

Pep:lip molar ratio	KI[a]	5-PCSL[b]	7-PCSL[b]	12-PCSL[b]
1:250	0.33	0.61	0.95	0.96
1:20	0.75	0.52	0.61	0.41
1:5	0.59	0.29	0.25	0.83

Fluorescence maximum intensity is recorded in 330–340 nm range. Quenching is calculated as ratio between the fluorescence intensity in the presence and in the absence of quencher for each peptide:lipid molar ratio.
[a] KI quencher is used to determine water exposed Trp residue with LUVs in solution.
[b] The doxyl-labeled lipid quenches Trp fluorescence in a distance dependent manner giving the depth of peptide penetration into vesicles.

4. Discussion

It is well known that cationic and hydrophobic residues of peptides and lipid composition of membranes are the factors that mainly affect the activity of AMPs [1–7]. HNP-1 has a positive net charge equal to +3, conferred by four cationic arginine residues and a single anionic glutamic acid residue [17,18,21]. The cationic nature of defensins suggests that their antimicrobial activity prevalently depends upon electrostatic interactions [19,20].

Large unilamellar vesicles (LUVs) resembling the composition of the *Escherichia coli* inner membrane have been used in this work. These vesicles have a more complex structure compared to simpler model membranes commonly used in other works and cardiolipin confers a negative charge and a rigid structure to the vesicle surface. [12,37,45,46]. The relative peptide:lipid molar ratio is another important aspect to evaluate the antimicrobial activity of a peptide. High concentrations of bound peptide are required for antimicrobial activity but AMPs that present activity and leakage only at a peptide:lipid molar ratio higher than 1:50 can be considered as experimental artefacts [45].

In the vast literature on pore-forming peptides, convincing evidences for specific three dimensional transmembrane pore structures is rare. Recently, a solid state NMR study has been performed to elucidate the three dimensional structure of the pores formed by the human HNP-1 peptide in DMPC:DMPG bilayer using a 1:18 peptide: lipid molar ratio [12]. This peptide concentration is far away from the ones of the biological activity.

In this work, the binding properties of HNP-1 with negative charged lipid phase has been examined with the aim to shed light on the overall mechanism of HNP-1-membrane interaction at different concentrations of peptide.

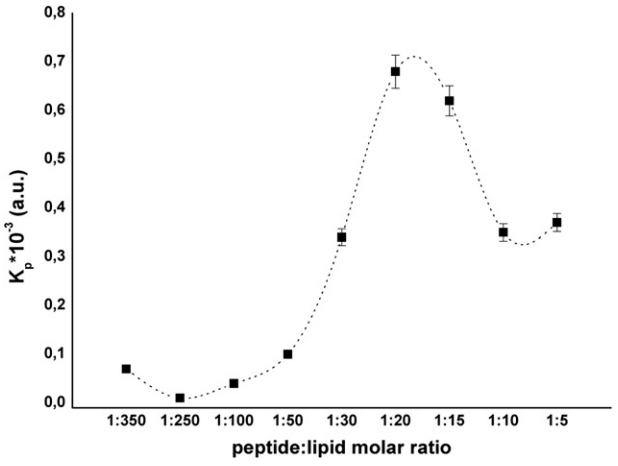

Fig. 5. Partition coefficients calculated for (1:350, 1:250, 1:100 and 1:50) and (1:30, 1:20, 1:15, 1:10 and 1:5) peptide:lipid molar ratios.

HNP-1 in its native form has a compact structure composed of three antiparallel β-sheet and a β-hairpin interconnected by three disulfide bonds. Furthermore, the crystal structure, as well as equilibrium sedimentation studies, suggests that defensins exist as dimers or higher multimers in solution [19,25]. The CD spectra of native defensins exhibit changes in the presence of increasing amount of lipids suggesting that a reorganization process takes place during phospholipid destabilization (Fig. 1). Indeed, a basket shape dimer with a polar top and an apolar base was resolved by crystal structure studies and proposed to translocate to membrane environment maintaining its dimeric structure [25]. The same behavior was also evidenced for other AMPs in previous studies [37,46].

The emission fluorescence spectra have given more interesting results. HNP-1 in solution reveals the maximum emission band at 343 nm, typical of a solvent exposed Trp. For 1:250 peptide:lipid molar ratio a decrease of fluorescence quantum yield paired with a shift of the emission band (332 nm) is recorded. In this condition Trp-26 is confined to the outer leaflet of the membrane and the peptide is partially associated to lipid bilayer.

Once the 1:20 HNP-1:LUVs ratio is reached, a large amount of defensin penetrates into the lipid bilayer as indicated by the blue shift (332 nm) of the emission band and the strong increase in quantum yield. In this condition, Trp is displaced to the apolar environment of the lipid phase. The same value of the Trp fluorescence was theoretically predicted by us for the residue in the apolar environment of a protein [47]. For high peptide:lipid molar ratio (1:5) the blue shift at 332 nm suggests an interfacial location of the Trp residue. These results are in perfect agreement with the EPR and quenching experiments. The EPR spectroscopy, in fact, is a powerful tool to evaluate the interaction and insertion of AMPs into pospholipid bilayer. The analysis of the changes in outer splitting constant of a spin-label nitroxyl radical anchored in a different position of the lipid bilayer allowed us to understand the ability of the peptide to penetrate into membranes. Our EPR data show that for 1:250 ratio no destabilization of the inner part of membrane is present, but only a weak interaction with 5-PCSL (data not shown) evidencing a poor binding with the membrane surface. On the other hand, an increase of the correlation time in the case of 12-PCSL has been recorded only for 1:20 peptide:lipid ratio. For high peptide:lipid molar ratio (1:5 and 1:10) HNP-1 interacts prevalently with 5-PCSL and in a lesser extent with 7-PCSL (Fig. 4 and Table 1). No variation for interaction with the 12-PCSL has been recorded for these two ratios (see correlation time, Table 2), emphasizing that the interaction is prevalently localized on the outer part of the bilayer, thus leading to phospholipid destabilization. From our EPR data we cannot clearly define the correct mechanism of pore formation at the threshold concentration (1:20), but the change in correlation time of 12-PCSL shows that the peptide penetrates into the bilayer in a membrane spanning-mode.

The partition coefficient and relative free energy values are well in agreement with the other data. The higher value for partition coefficient paired with the lower value for free energy has been recorded at the 1:20 molar ratio (Table 3). The experiments in the presence of

the water soluble quencher KI show that the peptide at low concentration (1:250) is placed on the surface with the Trp residue more exposed to solvent than at higher peptide concentration (1:5). At the threshold concentration (1:20) Trp is inserted into the lipid bilayer. The experiments with doxyl labeled-lipids show clearly that the interaction with 12-PCSL is exerted only at the peptide threshold condition. Considering this we can speculate that Trp, originally parallel oriented to membrane surface, penetrates into the bilayer changing its orientation in a manner with the indole moiety less exposed to water solution. At higher peptide concentrations (high peptide:lipid molar ratio) the α-defensin resides mainly on the bilayer surface, even if deeper inserted than for lower ratios, and the more suitable mechanism of action can be based on the non-specific "interfacial activity" leading to membrane-destabilizing effect altering the packing and organization of the lipids. [46,48,49].

5. Conclusion

Overall, this work provides further insights into the binding mode of the human α-defensin HNP-1 with negative phosholipid bilayer indicating that the mode of interaction is peptide concentration dependent.

For lower ratios (1:250–1:350), the most "physiological" concentrations, the activity is prevalently localized on membrane surface. This can bring to a thinning and destabilization of phospholipid bilayer. Increasing peptide concentration at 1:20 ratio the penetration and pore formation is the more suitable mechanism of action. This ratio represents the threshold concentration for the trans-membrane spanning mode. Strong membrane destabilization and partitioning of the peptide in the phospholipid bilayer is from the other hand presents for high peptide:lipid ratios (1:10–1:5).

This work can be useful to understand the mode of action of HNP-1 but at the same time can be considered as a model to demonstrate how the change in peptide concentration and the presence of a lipid membrane highly negatively charged can be crucial to define the biological activity for AMPs.

References

[1] H.G. Boman, Peptide antibiotics and their role in innate immune, Annu. Rev. Immunol. 13 (1995) 61–92.
[2] R.E.W. Hancock, D.S. Chapple, Peptide antibiotics, Antimicrob. Agents Chemother. 43 (1999) 1317–1323.
[3] M. Zasloff, Antimicrobial peptides of multicellular organism, Nature 415 (2002) 389–395.
[4] K.A. Brodgen, Antimicrobial peptides:pore formers or metabolic inhibitors in bacteria? Nat. Rev. Microbiol. 3 (2005) 238–250.
[5] H.P. Jessen, P. Hamill, R.E. Hancock, Peptide antimicrobial agents, Clin. Microbiol. Rev. 19 (2006) 491–511.
[6] K.V.R. Reddy, R.D. Yedery, C. Aranha, Antimicrobial peptides. Premises and promises, Int. J. Antimicrob. Agents 24 (2004) 536–547.
[7] M.R. Yeaman, N.Y. Yount, Mechanism of antimicrobial peptide: action and resistance, Pharmacol. Rev. 55 (2003) 27–54.
[8] R.M. Epand, H.J. Vogel, Diversity of antimicrobial peptides and their mechanism of action, Biochim. Biophys. Acta 1462 (1999) 11–28.
[9] M.N. Melo, R. Ferre, M.A.R.B. Castanho, Antimicrobial peptides: linking partition, activity and high membrane bound concentrations, Nat. Rev. Microbiol. 7 (2009) 245–250.
[10] H.W. Huang, Molecular mechanism of antimicrobial peptides: the origin of cooperativity, Biochim. Biophys. Acta 1758 (2006) 1292–1302.
[11] M.T. Lee, W.C. Hung, F.Y. Chen, H.W. Huang, Many-body effect of antimicrobial peptides: on the correlation between lipid's spontaneous curvature and pore formation, Biophys. J. 89 (2005) 4006–4016.
[12] Y. Zhang, W. Lu, M. Hong, The membrane-bound structure and topology of human α-defensin indicate a dimer pore mechanism for membrane disruption, Biochemistry 49 (2010) 9770–9782.
[13] S. Pistolesi, R. Pogni, J.B. Feix, Membrane insertion and bilayer perturbation by antimicrobial peptide CM15, Biophys. J. 93 (2007) 1651–1660.
[14] R.I. Lehrer, Primate defensin, Nat. Rev. Microbiol. 2 (2004) 727–738.
[15] W. Zhibin, L. Xiangquen, E. de Leeuw, B. Ericksen, L. Wuyuan, Why is the Arg^{5}-Glu^{13}salt bridge conserved in mammalian α-defensins, J. Biol. Chem. 52 (2005) 43039–43047.
[16] M. Edith, T. Ganz, R.I. Lehrer, Defensins and other endogenous peptide antibiotics of invertebrates, J. Leukocyte Biol. 58 (1995) 128–136.
[17] K. De Smet, R. Contreras, Human antimicrobial peptides: defensins, cathelicidins and histatins, Biotechnol. Lett. 27 (2005) 1337–1347.
[18] S.H. White, W.C. Wimley, M.E. Selsted, Structure, function and membrane integration of defensins, Curr. Opin. Struct. Biol. 5 (1995) 521–527.
[19] G. Fujii, M.E. Selseted, D. Eisenberg, Defensins promote fusion and lysis of negatively charged membranes, Protein Sci. 2 (1993) 1301–1312.
[20] M.R. Lourenzoni, A.M. Namba, L. Caseli, L. Degreve, M.E.D. Zaniquelli, Study of the interaction of human defensins with cell membrane models: relationships between structure and biological activity, J. Phys. Chem. 111 (2007) 11318–11329.
[21] G. Zou, E. de Leeuw, C. Li, M. Pazgier, C. Li, P. Zeng, W.Y. Lu, J. Lubkowski, W. Lu, Toward understanding the cationicity of defensin, J. Biol. Chem. 27 (2007) 19653–19665.
[22] L.A. Stevens, R.L. Levine, B.R. Gochuico, J. Moss, ADP-ribosylation of human defensin HNP-1 results in the replacement of the modified arginine with the noncoded amino acid ornithine, PNAS 106 (2009) 19796–19800.
[23] G. Wei, E. de Leeuw, C. Li, M. Pazgier, M. Rajabi, J. Li, G. Zou, G. Jung, W. Yuan, W.Y. Lu, R.I. Lehrer, W. Lu, Trp-26 imparts functional versatily to human α-defensin HNP-1, J. Biol. Chem. 285 (2010) 16275–16285.
[24] D.I. Chan, E.J. Prenner, H.J. Vogel, Tryptophan- and arginine-rich antimicrobial peptide: structures and mechanism of action, Biochim. Biophys. Acta 1758 (2006) 1184–1202.
[25] C.P. Hill, J. Yee, M.E. Selsted, D. Eisenberg, Crystal structure of Defensin HNP-3, an amphiphilic dimer: mechanisms of membrane permeabilization, Science 251 (1991) 1481–1485.
[26] W.C. Wimley, M.E. Selsted, S.H. White, Interaction between human defensin and lipid bilayer: evidence for formation of multimeric pore, Protein Sci. 3 (1994) 1362–1373.
[27] N.E. Good, G.D. Winget, W. Winter, T.N. Connolly, Hydrogen ion buffers for biological research, Biochemistry 5 (1966) 467–477.
[28] S. Lopes, C.S. Neves, P. Eaton, P. Gameiro, Cardiolipin, a key component to mimic *E. coli* bacterial membrane in model system revealed by dynamic light scattering and steady-state fluorescence anisotropy, Anal. Bioanal. Chem. 398 (2010) 1357–1366.
[29] J.C.M. Stewart, Colorimetric determination of phospholipids with ammonium ferrothiocyanate, Anal. Biochem. 104 (1980) 10–14.
[30] W.T. Heller, A.J. Waring, R.I. Lehrer, H.W. Huang, Multiple states of β-sheet peptide protegrin in lipid bilayers, Biochemistry 37 (1998) 17331–17338.
[31] A.S. Ladokhin, S. Jayasinghe, S.H. White, How to measure and analyze tryptophan fluorescence in membrane properly, and why bother? Anal. Biochem. 285 (2000) 235–245.
[32] B. Christianes, S. Symoens, S. Vanderheyden, Y. Englborghs, A. Joliot, A. Prochiants, J. Vandekerckhove, M. Rosseneu, B. Vanloo, Tryptophan fluorescence study of the interaction of penetrating peptides with model membranes, Eur. J. Biochem. 269 (2002) 2918–2926.
[33] Y. Groemping, N. Hellmann, Spectroscopic methods for the determination of protein interaction, Curr. Protoc. Protein Sci. (2005), http://dx.doi.org/10.1002/0471140864.ps2008s39.
[34] D.A. Allende, A. Vidal, S.A. Simon, T.J. McIntosh, Bilayer interfacial properties modulate the binding of amphipathic peptides, Chem. Phys. Lipids 122 (2003) 65–76.
[35] A.S. Landokhin, M.E. Selsted, S.H. White, Bilayer interaction of indolicidin, a small antimicrobial peptide rich in tryptophan, proline and basic amino acids, Biophys. J. 72 (1997) 794–805.
[36] S.H. White, W.C. Wimley, A.S. Ladokhin, K. Hristova, Protein folding in membranes: determining energetics of peptide–bilayer interactions, Methods Enzymol. 295 (1998) 62–87.
[37] J.M. Rausch, R.J. Marks, R. Rathinakamur, W.C. Wimley, β-Sheet pore-forming peptides selected from a rotational combinatory library: mechanism of pore formation in lipid vesicles, Biochemistry 46 (2007) 12124–12139.
[38] L.P. Liu, C.M. Deber, Anionic phospholipids modulate peptide insertion into membranes, Biochemistry 36 (1997) 5476–5482.
[39] F.Y. Chen, M.T. Lee, H.W. Huang, Evidence for membrane thinning effect as the mechanism for peptide induced pore formation, Biophys. J. 84 (2003) 3751–3758.
[40] M. Mandal, R. Nagaraj, Antibacterial activities and conformations of synthetic α-defensin HNP-1 and analogs with one, two and three disulfide bridges, J. Pept. Res. 59 (2002) 95–104.
[41] G. D'Errico, A.M. D'Ursi, D. Marsh, Interaction of a peptide derived from glycoprotein gp36 of feline immunodeficiency virus and its lipoylated analogue with phospholipid membranes, Biochemistry 47 (2008) 5317–5327.
[42] S. Pistolesi, L. Rossini, E. Ferro, R. Basosi, L. Trabalzini, R. Pogni, Humanin structural versatility and interaction with model cerebral cortex membranes, Biochemistry 48 (2009) 5026–5033.
[43] M. Ramakrishnan, P.H. Jensen, D. Marsh, α-Synuclen association with phosphatidylglycerol probed by lipid spin labels, Biochemistry 42 (2003) 12919–12926.
[44] A. Falanga, R. Tarallo, G. Vitiello, M. Vitiello, E. Perillo, M. Cantisani, G. D'Errico, M. Galdiero, S. Galdiero, Biophyscal characterization and membrane interaction of two fusion loops of glycoprotein B from herpes simplex type I virus, PLoS One 7 (2012), http://dx.doi.org/10.1371/journal.pone.0032186.
[45] W.C. Wimley, Describing the mechanism of antimicrobial peptide action with the interfacial activity model, ACS Chem. Biol. 10 (2010) 905–917.
[46] R. Rathinakamur, W.C. Wimley, Biomolecular engineering by combinatorial design and high-toughput screening: small soluble peptide that permeabilize membranes, J. Am. Chem. Soc. 130 (2008) 9849–9858.
[47] S. Pistolesi, A. Sinicropi, R. Pogni, R. Basosi, N. Ferrè, M. Olivucci, Modeling the fluorescence of protein-embedded tryptophans with ab initio multiconfigurational

quantum chemistry: the limiting case of parvalbumin and monellin, J. Phys. Chem. B 49 (2009) 16082–16090.
[48] H.W. Huang, Action of antimicrobial peptide: two state model, Biochemistry 39 (2000) 8348–8352.
[49] R. Rathinakamur, W.F. Walkenhorst, W.C. Wimley, Broad-spectrum antimicrobial peptides by rational design and high-throughput screening: the importance of interfacial activity, J. Am. Chem. Soc. 131 (2009) 7609–7617.